Unifying iteration rule for fractal objects

1997 J. Phys. A: Math. Gen. 30 1887

(http://iopscience.iop.org/0305-4470/30/6/015)

J. Phys. A: Math. Gen. **30** (1997) 1887–1896. Printed in the UK PII: S0305-4470(97)77181-6

Unifying iteration rule for fractal objects

A Kittel†, J Parisi†, J Peinke†, G Baier‡, M Klein‡ and O E Rössler‡

† Physical Institute, University of Bayreuth, D-95440 Bayreuth, Germany

‡ Institute for Physical and Theoretical Chemistry, University of Tübingen, D-72076 Tübingen, Germany

Received 15 August 1996, in final form 7 January 1997

Abstract. We introduce an iteration rule for real numbers capable to generate attractors with dragon-, snowflake-, sponge-, or Swiss-flag-like cross sections. The idea behind it is the mapping of a torus into two (or more) shrunken and twisted tori located inside the previous one. Three distinct parameters define the symmetry, the dimension, and the connectedness or disconnectedness of the fractal object. For some selected triples of parameter values, a couple of well known fractal geometries (e.g. the Cantor set, the Sierpinski gasket, or the Swiss flag) can be gained as special cases.

1. Introduction

The concept of fractality has gained considerable importance to grasp a variety of different structures in nature [1–3]. Whereas iterated function systems are known to produce ferns and trees, the shape of coast lines, clouds, cancer etc and are characterized by their fractal dimensions. As reported elsewhere [4–7], fractal behaviour can be interpreted as being originally produced by an instability and a chaotic mixing. Therefore, the fractality of an object can be tuned by the ratio of two parameters. Compared with the richness of different forms observed in nature, the characterization by only determining the fractal dimension is a crude simplification. Hereto, Mandelbrot [1] has proposed to introduce a further measure called 'lacunarity' providing additional information about the shape. A further classification of a structure concerns its symmetry.

In the present paper, we introduce a new iteration rule that is able to produce fractal objects with different symmetry, lacunarity, and fractal dimension which are either connected or disconnected. The set of objects generated even embraces fractal objects well known from other iteration rules. Our paper is organized as follows. In section 2, the iteration rule is introduced. Section 3 describes an alternative numerical algorithm to determine the fractal cross sections and their blow-up. Sections 4 and 5 give some selected examples of cross sections with different symmetry.

2. The iteration rule

In order to capture the attractor geometry, we propose an elementary iteration rule that is able to generate different complex fractals under variation of three control parameters. We deal with a fractal structure generated by mapping a torus (in the (x, y, z) space)† into two

† Note that tori are chosen only for convenience. In general, it is completely equivalent to use any shrinking object characterized via only one parameter.

0305-4470/97/061887+10$19.50

or more shrunken and twisted tori completely lying inside the former one. The mapping process is applied again to the tori created by the previous step, and so on. Obviously, after n steps we have m^n tori. Here m denotes the number of shrunken tori. In the case of nonoverlapping tori, their cross section develops as $\pi a^2 m^n$, where parameter a determines the contraction strength. The equation for the nth level ($n = 1, \ldots, \infty$) and for the lth torus ($l = 1, \ldots, m^n$) reads as follows:

$$\begin{aligned} x_l &= \cos(\varphi)\left[b + a^n \cos\gamma + \sum_{i=1}^{n} a^{(i-1)}(1-a)\sin\left(i\varphi + \frac{2\pi k_{li}}{m}\right)\right] \\ y_l &= \sin(\varphi)\left[b + a^n \cos\gamma + \sum_{i=1}^{n} a^{(i-1)}(1-a)\sin\left(i\varphi + \frac{2\pi k_{li}}{m}\right)\right] \\ z_l &= a^n \sin\gamma + \sum_{i=1}^{n} a^{(i-1)}(1-a)\cos\left(i\varphi + \frac{2\pi k_{li}}{m}\right) \end{aligned} \tag{1}$$

with the parametric representation of the torus by the angle variables $\varphi, \gamma \in [0, 2\pi[$. b denotes the larger radius and a denotes the contraction parameter of the smaller radius. The m^n different tori are separated by the last term of the r.h.s. of equation (1). It contains a sum with the running index i over the parameter $k_{li} = 0, \ldots, (m-1)$ in the trigonometric term of angle φ. The term $i\varphi$ causes a twisting of the tori that increases linearly with the iteration depth. k_{li} can be seen as a digit which belongs to one of the m^n possible n-tuples of the variation. Thus, the lth torus of the nth level is characterized by the n-tuple $k_l = \{k_{l1}, k_{l2}, \ldots, k_{ln}\}$. Note that, in any case, the n-tuple must be identical in all three equations (x, y, z). The first two steps of the underlying process (i.e. for $m = 2$ and $n = 0, 1, 2$) are illustrated in figure 1. For enlightenment, the three control parameters involved operate as follows: The first one, denoted by m, fixes the symmetry of the attractor cross section (thus, called symmetry parameter). The second one, denoted by a, yields the degree of contraction as to decide whether the cross section is connected or not (thus, called contraction parameter). The third one, denoted by φ, gives the angle related to the x-axis at which the intersection along the z-axis takes place (thus, called intersection angle).

So far, the proposed mapping process seems to be similar to the well known solenoid map introduced by Smale [8]. The fundamental difference lies in the topology of the nth iterate. For the case of the Smale solenoid, there arises only one twisted torus. As a consequence of the Moebius-band-like mapping process, the period length of the nth iterate is 2^n of the initial length (period doubling). To describe the Smale solenoid, formula (1) has to be changed in the following way: the summation is replaced by a simple trigonometric term with the argument $\varphi/2^n$, i.e. the twisting of tori decreases with the iteration depth. In our case, the nth iterate consists of n independent tori, each one keeping the initial period length. Note that the n tori do not relate to a trajectory in phase space. Nevertheless, we call the final structure for $n \to \infty$ an 'attractor'.

Let us now focus on the influence of the contraction parameter a. For example, in the case of $m = 2$ and $a \leqslant \frac{1}{2}$, the tori are totally separated. For $m = 2$ and $a > \frac{1}{2}$, they penetrate one another. Apparently, parameter a determines the dimension of the attractor, i.e. the dimension increases with increasing a. The cross sections (in analogy to Poincare sections) of attractors are defined by the set of intersection points of the plane of constant angle φ. To give a vivid idea, the cross sections are nothing else but the set of intersection points of the object with a half plane limited by the z-axis and, in addition, defined by the intersection angle φ. Depending on the parameters m, a and φ, we observe a variety of fractal, self-similar objects. Those contain some well known structures such as the Cantor set ($m = 2$, $a = \frac{1}{3}$, and $\varphi = 0$) or the Sierpinski gasket ($m = 3$, $a = \frac{1}{2}$, and $\varphi = 0$).

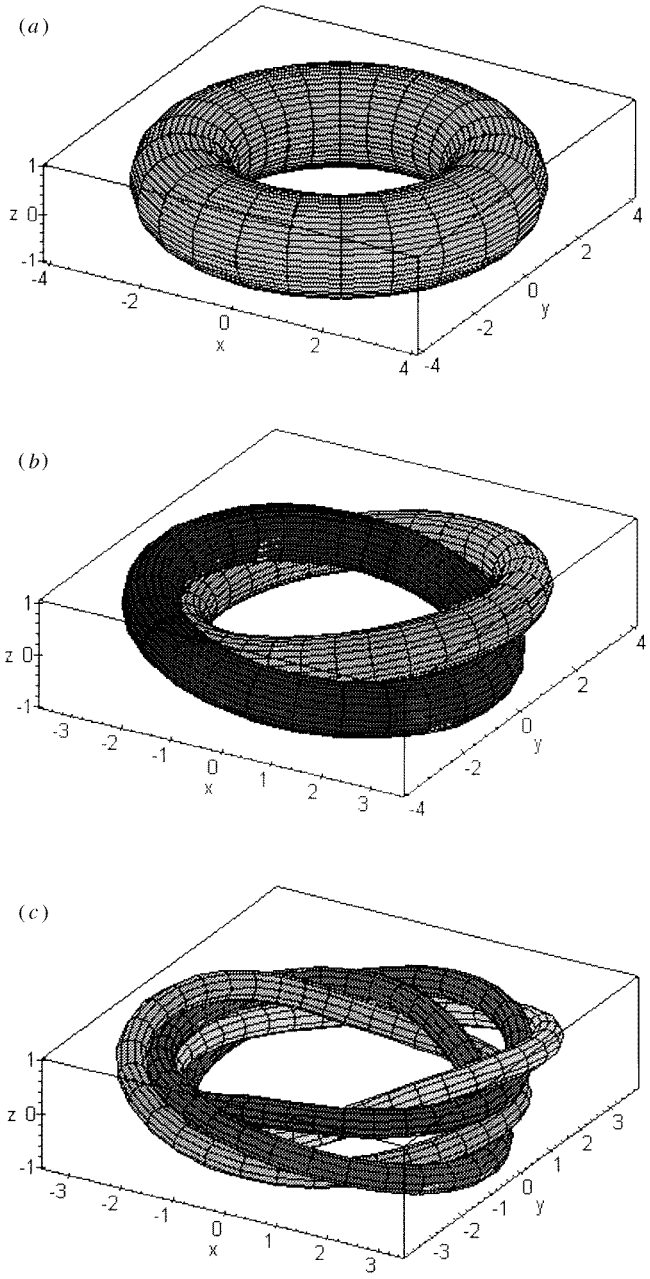

Figure 1. Surface plots in the (x, y, z) space of a torus (a) iterated to two tori (b) and, after a further iteration, to four tori (c).

The fractal dimension of the resulting cross section is determined by only two of the parameters, namely, the symmetry m and the contraction parameter a. For small values of a, the fractal dimension can be evaluated as

$$d_f = \frac{\log m}{\log 1/a} \tag{2}$$

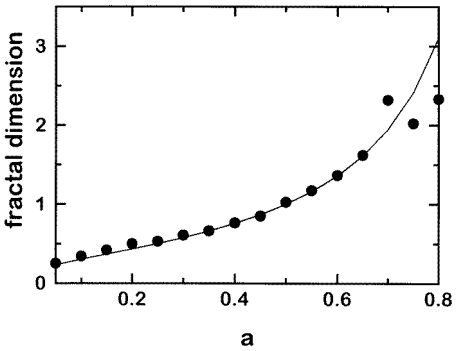

Figure 2. Fractal dimension versus contraction parameter determined numerically for the case $m = 2$, $\varphi = 30$ (dotted curve) and gained from equation (2) (full curve). The fractal dimension, of course, has to saturate at a value of two. The deviation of the points of the numerically evaluated dimensions for $a \geqslant 0.7$ are due to numerical uncertainties.

as shown in figure 2 for an exemplary case. For larger values, the fractal dimension of the cross section saturates at the value of two where tori of different iteration paths overlap. The effect of saturation sensitively depends on the values of all three parameters.

3. The numerical algorithm

For obtaining different cross sections of an attractor in a general approach, there are three alternative paths. First, one can apply the iteration rule to an arbitrarily chosen initial value. After having passed a transient, the iteration delivers points of the attractor. As a consequence of the assumption of ergodicity, the approximated cross section can be generated by taking a large enough number of iterations. Such a brute force technique has the disadvantage of demanding a huge number of iterations for calculating a blow-up of the cross section. Secondly, during the iteration process, we put m disks shrunken by the factor a with a shifted centre inside the former ones. Again, the same disadvantage arises for a blow-up of the cross section. While these two methods always calculate the whole section even if one is interested in a blow-up only, there exists a third numerical algorithm which overcomes that problem.

Hereto, we apply the basic idea used to uncover the famous Julia and Mandelbrot sets. Instead of dealing with an attractor, our system is inverted to a repeller, i.e. the parameter of contraction, a, changes into a parameter of expansion, $1/a$. Of course, the direction of the shift during iteration must be reversed. Points belonging to the cross section of the attractor are identified by the fact that they do not leave the circle of unity under an infinite number of (inversed) iteration. For that case, we are able to discriminate the cross section of the attractor by scanning an area of initial values. A possible visualization of the neighbourhood of the attractor is to colour each point representing an initial value in accordance with the number of iterations which are necessary to leave the circle of unity.

Our iteration rule when subject to the coordinates $r = \sqrt{x^2 + y^2}$ and z looks as follows:

$$r_{n+1} = \frac{r_n - 1 + a - (1-a)\sin\varphi}{a}$$
$$z_{n+1} = \frac{z_n + (1-a)\cos\varphi}{a} \tag{3}$$

with $\varphi = \arctan(y/x)$. The radii (both equal unity) are chosen such that the initial torus

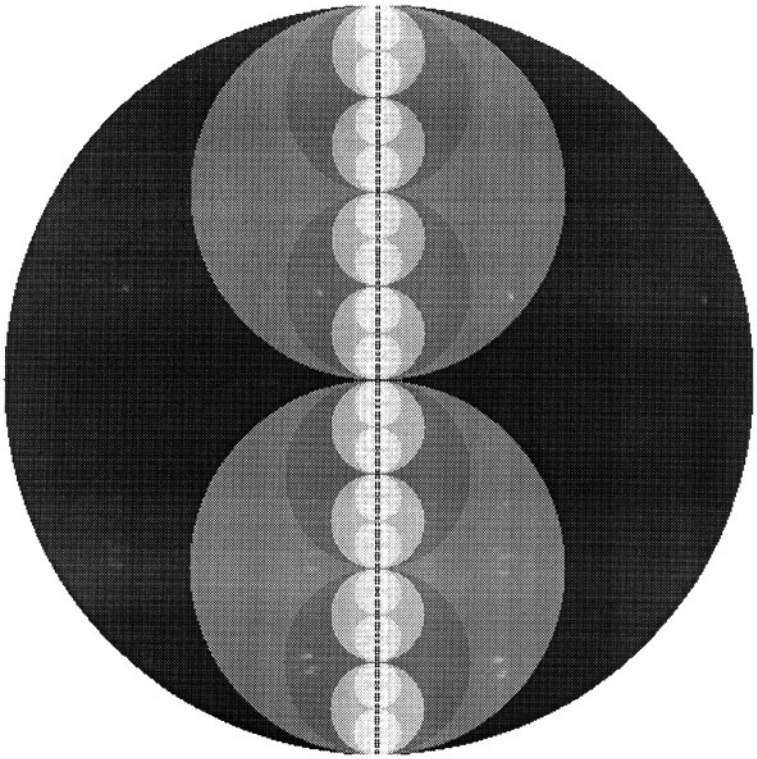

Figure 3. Plane of initial values of the coordinates r and z coloured according to the iteration depth (for details, see text). (*a*) Parameters: $m = 2$, $a = \frac{1}{2}$, and $\varphi = 0$; window: r from 0 to 2, z from -1 to 1. (*b*) Parameters: $m = 2$, $a = 1/\sqrt{2}$, and $\varphi = 30°$; window: r from 0 to 2, z from -1 to 1. (*c*) Blow-up of (*b*); window: r from 0.566 75 to 0.597 15, z from 0.537 35 to 0.567 75.

lies around the z-axis of the (x, y, z) space and also touches the origin. Note, however, one complication. As mentioned above, if the parameter a exceeds the value $\frac{1}{2}$, the tori intersect, i.e. the disks representing the cross section of the tori overlap. There exists an area of initial values which belongs to more than one disk. For convenience, we now restrict ourselves to the case $m = 2$ (later, to the cases $m = 3$, 4, 5, and 6), without loss of generality. Each disk represents one path of iteration in a binary tree. The overlap of different disks leads to an uncertainty of the path. We, therefore, have to check all possible paths, in order to end up with the correct (i.e. the largest) number of iterations for escape.

4. Cross sections of twofold symmetry

Figure 3 gives the (r, z) plane of initial values coloured according to the number of iterations which are necessary to leave the circle of unity. While the parameter m was kept constant ($m = 2$), examples for different values of the parameters a and φ are illustrated. Part (*a*) exhibits the case where the cross section of the attractor is simply connected and has the form of a straight line ($a = \frac{1}{2}$ and $\varphi = 0$). Part (*b*) shows a dragon-like cross section that again is simply connected, but has a totally perforated structure ($a = 1/\sqrt{2}$ and $\varphi = 30°$). Finally, part (*c*) displays a blow-up of part (*b*).

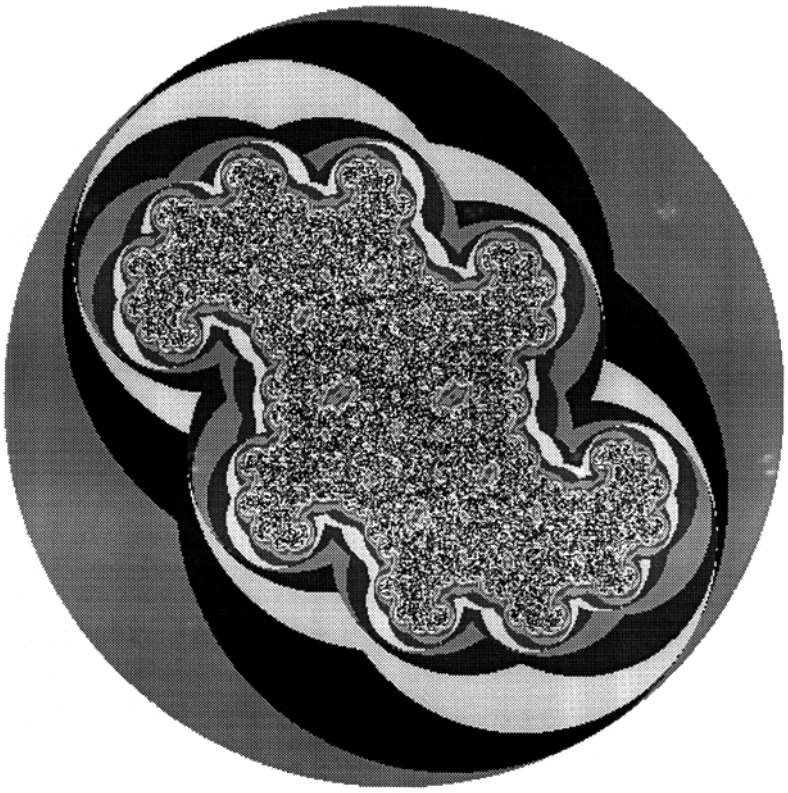

Figure 3. (Continued)

Next, we turn to the variety of structures generated by the iteration process. For clarifying the actual shape of the cross sections of the attractor, we change the display mode. That is, only points corresponding to initial values whose number of iterations for escape exceeds the value of 50 are coloured black. Figure 4 shows examples of different shapes in the (r, z) plane of initial values obtained for $m = 2$ and different values of a and φ. Part (a) represents the cross section of the attractor for the case of the same parameter values as chosen in figure 3(b). Here (in figure 4(a)), the cross section is simply connected, in contrast to the situation illustrated in figure 4(b) where it is totally disconnected. There (in figure 4(b)), parameter a is lowered from $1/\sqrt{2}$ to 0.68, whereas the section angle is kept constant at $\varphi = 30^\circ$. Figures 4(c) and (d) are further examples of connected attractor cross sections, the shape of which resembles a snowflake ($a = 1/\sqrt{2}$ and $\varphi = 60^\circ$) and an irregular sponge ($a = 1/\sqrt{2}$ and $\varphi = 80^\circ$), respectively. Note that these special fractals (for $m = 2$) have been previously observed elsewhere [3] by analysing a complex iterated function system†. There, we find a detailed discussion on connectivity. In case of the parameter set $a = 1/\sqrt{2}$ and $\varphi = 90^\circ$, the situation is similar to that given at $a = \frac{1}{2}$ and $\varphi = 0$ (see figure 3(a)), i.e. the structure is connected without any perforation. The difference lies in the fact that the former case excels by a compact rectangular form (representing a two-dimensional object), while the latter case ends up with a straight line

† While Barnsley uses a randomly driven switch for the sign of the iterated function system, our algorithm directly evaluates all relevant paths of the binary tree.

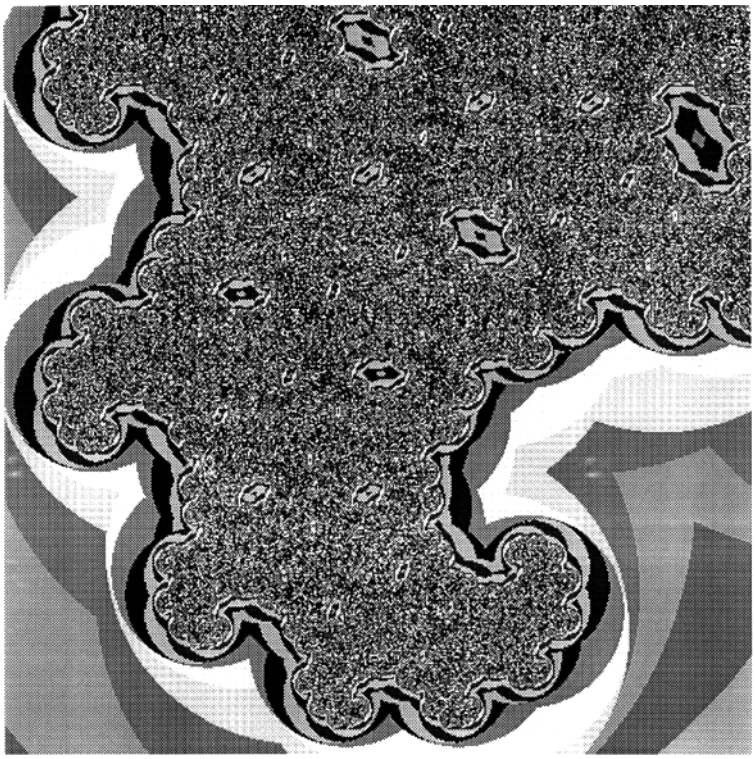

Figure 3. (Continued)

(representing a one-dimensional object). For arriving at another well introduced fractal geometry, the so-called Swiss flag (for more details, see [9]), we have fixed parameter a at the value 0.69 in figure 4(e).

5. Cross sections of higher symmetry

According to the display mode used in figure 4, figure 5 exhibits further examples of cross sections in the (r, z) plane of initial values obtained for $m > 2$ and different values of a and φ. The iteration depth is chosen to be 10 (instead of 50, as in figure 4). Part (a) shows the well known Sierpinski gasket for the parameter set $m = 3$, $a = \frac{1}{2}$, and $\varphi = 0$, part (b) shows the case for $\varphi = 60^\circ$ and unchanged other parameters. The quadratic Swiss flag in part (c) is calculated at $m = 4$, $a = 0.48$, and $\varphi = 0$, in part (d) analogously at $m = 4$, $a = 0.45$, and $\varphi = 60^\circ$. Eventually, parts (e) and (f) represent examples of higher symmetry gained at the parameter values $m = 5$, $a = 0.4$, $\varphi = 0$ and $m = 6$, $a = 0.4$, $\varphi = 0$, respectively.

6. Conclusion

We have introduced an algorithm of an iteration rule for real numbers capable of generating a wide variety of attractor cross sections. Their structure can be either connected or disconnected as well as perforated or not—so far demonstrated by visualization. None the less, they all have a self-similarity in common with different types of symmetry.

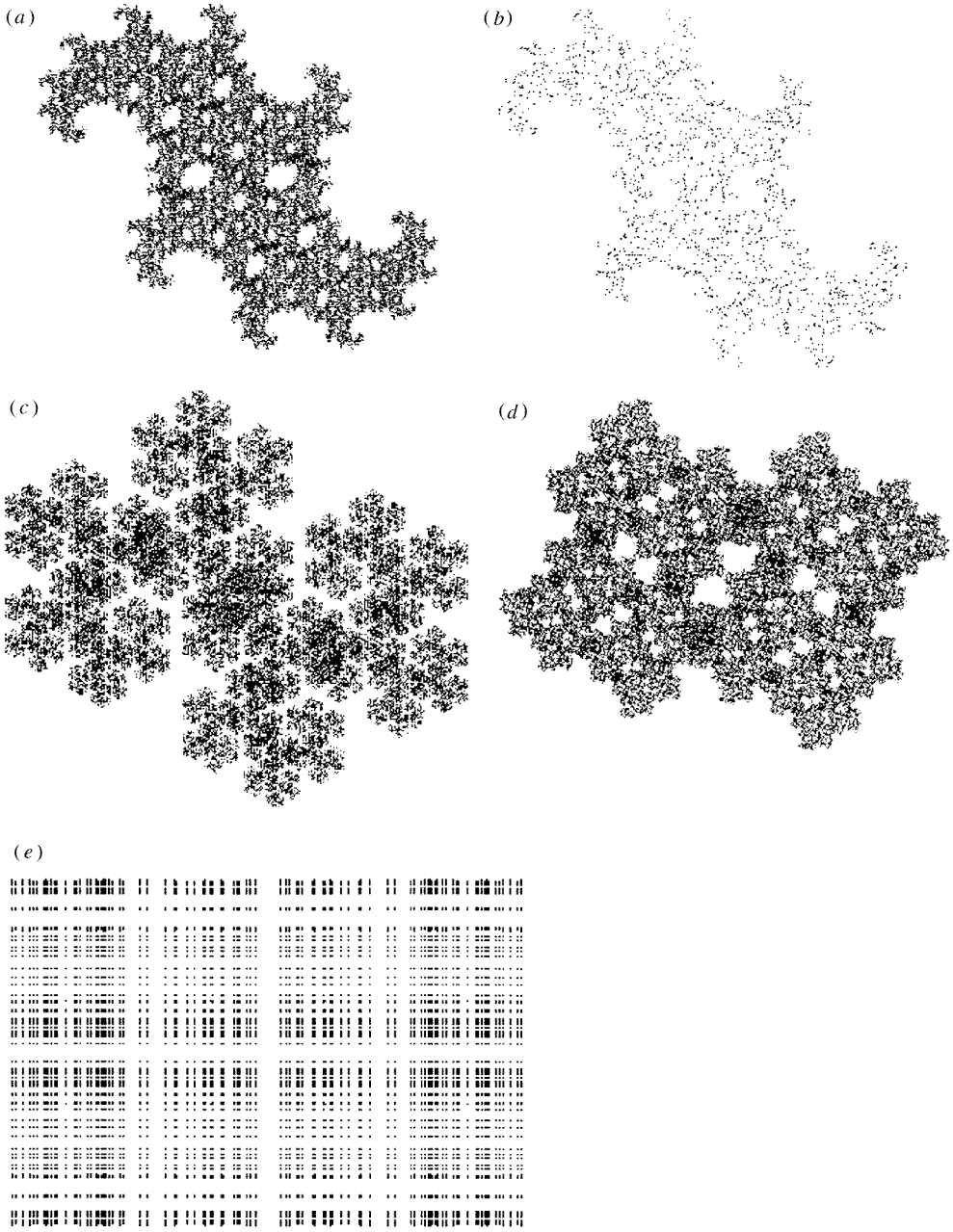

Figure 4. Plane of initial values of the coordinates r and z with points coloured black for an iteration depth larger than 50. (*a*) Parameters: $m = 2$, $a = 1/\sqrt{2}$, and $\varphi = 30^\circ$. (*b*) Parameters: $m = 2$, $a = 0.68$, and $\varphi = 30^\circ$. (*c*) Parameters: $m = 2$, $a = 1/\sqrt{2}$, and $\varphi = 60^\circ$. (*d*) Parameters: $m = 2$, $a = 1/\sqrt{2}$, and $\varphi = 80^\circ$. (*e*) Parameters: $m = 2$, $a = 0.69$, and $\varphi = 90^\circ$. All windows: r from 0 to 2, z from -1 to 1.

Our algorithm possesses the advantage to colour the actual iteration depth and, hence, to discriminate the neighbourhood of the attractor. Furthermore, any blow-up can be calculated

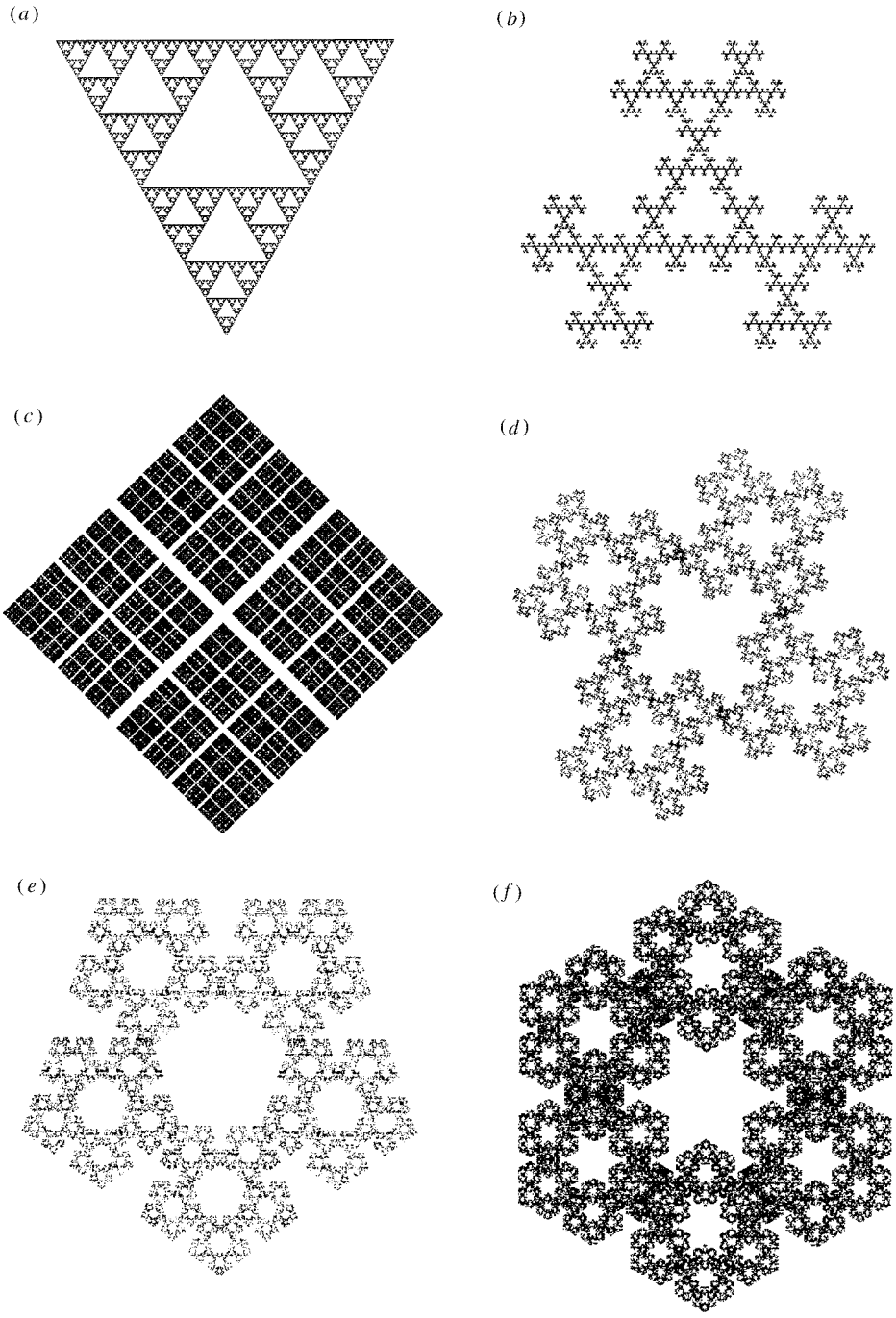

Figure 5. Plane of initial values of the coordinates r and z with points coloured black for an iteration depth larger than 10. (*a*) Parameters: $m = 3$, $a = \frac{1}{2}$, and $\varphi = 0$. (*b*) Parameters: $m = 3$, $a = \frac{1}{2}$, and $\varphi = 60^\circ$. (*c*) Parameters: $m = 4$, $a = 0.48$, and $\varphi = 0$. (d) Parameters: $m = 4$, $a = 0.45$, and $\varphi = 60^\circ$. (*e*) Parameters: $m = 5$, $a = 0.4$, and $\varphi = 0$. (*f*) Parameters: $m = 6$, $a = 0.4$, and $\varphi = 0$. All windows: r from 0 to 2, z from -1 to 1.

easily. The present method has the potential to analyse the attractor of any dynamical system, provided its cross section is the aim of interest. Moreover, one can perceive the calculus as a mathematical operation that projects the set of initial values to the set of points belonging to the cross section of the attractor. Certainly, the underlying mechanism possesses a wide universality in the sense that the class of created structures exceeds those gained by complex-analytic functions which, for example, are restricted to a twofold symmetry.

References

[1] Mandelbrot B B 1983 *The Fractal Geometry of Nature* (New York: Freeman)
[2] Peitgen H-O and Richter P H 1986 *The Beauty of Fractals* (Berlin: Springer)
[3] Barnsley M 1988 *Fractals Everywhere* (San Diego, CA: Academic)
[4] Peinke J, Klein M, Kittel A, Okninsky A, Parisi J and Rössler O E 1993 *Phys. Scr.* T **49** 672
[5] Beck C 1994 *Phys. Rev.* E **49** 3641
[6] Klein M, Kittel A and Baier G 1993 *Z. Naturforsch.* a **48** 666
[7] Baier G, Kittel A and Klein M 1993 *Phys. Rev.* E **48** 3409
[8] Smale S 1967 *Bull. Am. Math. Soc.* **73** 747
[9] Rössler O E, Kahlert C, Parisi J, Peinke J and Röhricht B 1986 *Z. Naturforsch.* a **41** 819